공학석사 학위논문

# Evaluation of an Off-Road Tracked Vehicle Performance Based on Soil-Track Interaction

# Soil-Track Interaction 을 고려한 야지구동 궤도차량의 구동성능 평가

**2016년 2월**


서울대학교 대학원

건설환경공학부

정 혜 민

# Evaluation of an Off-Road Tracked Vehicle Performance Based on Soil-Track Interaction

**Soil-Track Interaction** 을 고려한

야지구동 궤도차량의 구동성능 평가

지도 교수 정 충 기

이 논문을 공학석사 학위논문으로 제출함

**2016년 1월**

서울대학교 대학원

건설환경공학부

정 혜 민

정혜민의 공학석사 학위논문을 인준함

**2016년 2월**

위 원 장 _____ (인)

부위원장 _____ (인)

위 원 _____ (인)

# Abstract

## Evaluation of an Off-Road Tracked Vehicle Performance Based on Soil-Track Interaction

Jeong, Hye-Min
Department of Civil and Environmental Engineering
The Graduate School
Seoul National University

Off-road vehicles are widely used in the military, construction, and agriculture industries, and the demand especially for off-road tracked vehicles is increasing due to the recent expansion of the subsea construction market. Low ground contact pressure and settlement are necessary to realize sufficient traction for heavy (up to 20-ton) tracked vehicles.

Generally, the displacement of a vehicle running on a paved road equals the track displacement. As such, the vehicle's tractive performance relies mainly on its engine power. The displacement of a vehicle running off-road, however, equals the difference between the track displacement and the slip displacement. As such, the vehicle's tractive performance does not solely rely on its engine power. From this perspective, the tractive performance potential of an off-road tracked vehicle is limited by the soil thrust determined from the soil-track interaction. Most of the relevant studies that have been carried out,

however, did not take soil-track interaction into consideration. Further, the existing theoretical models (e.g., thrust-slip displacement) do not sufficiently consider important parameters, including the shear strength parameters and the track system configuration. Especially, as the soil thrust is the traction force induced on the bottom and sides of the track, both thrusts need to be investigated for the prediction of the tractive performance. Nevertheless, the side thrust generated by the grouser, which becomes more significant with the increase of the grouser height, was not fully understood and theoretically defined in the previous theoretical models for the soil thrust-slip displacement relationship.

In this study, a model track test was designed and then verified through a track model test to evaluate the off-road tracked vehicle performance. A series of model track tests were performed on a model track made of stainless steel to examine its side thrust. Gwan-ak weathered residual soil with a 40% relative density was trimmed into both a soil channel and a soil block to separate the side thrust from the total soil thrust. A model track was placed on the soil channel or soil block, and it was subjected to a surcharge mass and a lateral load corresponding to the vehicle weight and soil thrust, respectively. Based on the test results, the side thrust-slip displacement relationship and the failure surface on the side were evaluated and compared with the previous theoretical models.

**Keywords: Off-road tracked vehicle, Tractive performance, Soil-track interaction, Soil thrust, Side thrust**

**Student Number: 2014-20550**

# Contents

# List of Tables

# List of Figures

# Chapter 1 Introduction

## 1.1 Background

The demand for off-road tracked vehicles is increasing as they are effective on both soft and weak ground. Thus, adequate traction or tractive performance is a fundamental requirement of off-road vehicles. According to Wong and Huang (2006), the shearing behavior of the terrain is one of the major factors determining the tractive performance of an off-road tracked vehicle. The displacement of a vehicle running off-road, however, equals the difference between the track displacement and the slip displacement. An off-road tracked vehicle's tractive performance does not solely rely on its engine power and is limited by the soil thrust determined from the soil-track interaction. Thus, the tractive performance of an off-road tracked vehicle is evaluated based on the soil thrust-slip displacement, in which shearing action takes place on the soil-track interaction. In other words, the evaluation of the soil thrust-slip displacement relationship is a key factor for assessing the off-road vehicle performance and is a function of the shear strength parameters of the soil and track system configuration.

The evaluation methods of the tractive performance of an off-road tracked vehicle started to be developed in the 1950s. The most widely used method is the shear plane theory, which was defined as a function of slip displacement, adopting the Mohr-Coulomb criterion suggested by Wong (1956). Park et al.

(2000) assessed the bottom thrust, which is generated on the bottom of the track on the soil-track surface, and the side thrust, which is generated by the grouser, using Rankine's active earth pressure theory. Grečenko (2007) assessed the soil thrust exerted by soil block compression accompanied by frictional force based on the sheared-off parts and slides along the soil-track interface after the transition point. Even though the soil thrust consists mainly of the bottom thrust and the side thrust, the previous research had limitations in considering the side thrust, which is generated by the grouser. Although experimental studies have actually been performed on a variety of track shapes, most of the studies did not consider the soil-track interaction and simply evaluated the soil thrust (traction) changes according to the track and grouser shape.

In this study, the soil thrust was evaluated considering the soil condition, track and grousers, etc. In addition, the side thrust-slip displacement relationship was focused on and was compared with the previous theoretical models.

## 1.2 Objectives & Scope of This Study

This dissertation deals with the evaluated off-road tracked vehicle performance based on soil-track interaction. A model track was placed on soil channel or soil block and subjected to surcharge mass and lateral load corresponding to vehicle weight and soil thrust, respectively. From the test results, side thrust and slip displacement relationship and failure surface on the side were evaluated and compared with previous theoretical models. The specific objectives of this study are as follows:

1. Design and verification of track model test to evaluate the off-road tracked vehicle performance: soil block with relative densities of 40% so as to separate side thrust from total soil thrust.
2. Assessment of soil thrust as the sum of bottom thrust and side thrust based on shear plane theory (Bekker, 1956).
3. Evaluation of side thrust from the track model test results: from the test results, side thrust and slip displacement relationship and failure surface on the side were evaluated and compared with previous theoretical models.

## 1.3 Dissertation Organization

This dissertation documents evaluate an off-road tracked vehicle performance based on soil-track interaction.

**Chapter 1.Introduction**

Introduction includes research background and objectives, and dissertation organization was described.

**Chapter 2.Literature Review**

Literature review for methodology to the development and evaluation of off-road vehicles and existing theoretical model of tractive performance are described.

**Chapter 3.Experimental Program**

The experimental concept, testing chamber, testing material are described

**Chapter 4.Experimental Results and Analysis**

Based on experimental results soil thrust-slip displacement curve fitted with theoretical model. And the coefficient of earth pressure $K_s$ is provided for evaluate the side thrust

## Chapter 5.Conclusions and Recommendations

Summary and conclusions for this study are described and recommendations for the further study are presented.

# Chapter 2 Literature Review

## 2.1 Introduction

The evaluation of tractive performance of off-road tracked vehicle has been developed in 1950s. Especially, the publication of Dr M.G. Bekker's classic treatises, Theory of Land Locomotion in 1956 and Off-the-Road Locomotion and Introduction to Terrain-Vehicle Systems in the 1960s, stimulated a great deal of interest in the systematic development of the principles of land locomotion mechanics (Bekker, 1956, 1960, 1969).

In early days, the development of tractive performance has been guided by empirical method like as VCI method or MMP method. However these methods are uncertain whether empirical equations based on filed test data collected prior to 1960s. Also it is inability to predict the influence of terrain characteristics. In other words, these are lack of consideration for important parameters such as track-system configuration of soil shear parameters.

Secondly, Method for theory of plastic equilibrium (Wong, 1989; Wong and Reece, 1966; Karafiath and Nowatzki, 1978) is modeling the terrain as a rigid, perfectly plastic material so as used to specify the boundary conditions which is primarily based on empirical data and simplifying assumption. However the behavior of natural terrains does not conform to a rigid and perfectly plastic material, especially soft terrain. So it is not capable of predicting the deformation of the soil caused by vehicular load.

One of the better known methods for parametric analysis of tracked vehicle performance is that originally developed by Bekker (1956). Bekker(1956) discuss in shear plane theory, shear stress (soil thrust) was defined as a function of slip displacement, obeyed the Mohr-Coulomb criterion. And other method is Compression-Sliding approach which suggested by Grečenko (2007). In Compression-Siding approach, soil thrust exerted by soil block compression accompanied by frictional force (compassion stage). And then, soil block is sheared off and slides along the soil-track interface after the transition point (sliding stage). The method for parametric analysis is evaluate the total soil thrust sum of the soil thrust generated by each single grouser. So this method is useful to consider each force which effect the tracked vehicle.

In this study, assessment of soil thrust based on parametric analysis especially, shear plane theory (Bekker, 1956).

## 2.2 Traveling Mechanism of Off-Road Tracked Vehicle

Generally, displacement of vehicle which travels paved road equals to track displacement (Figure 2.1). So, tractive performance relies mainly on engine power. However, displacement of vehicle which travels off-road equals to the difference between track displacement and slip displacement (Figure 2.2). In other words, an off-road tracked vehicle's tractive performance does not solely rely on engine power and limited by the soil thrust determined from soil-track interaction.

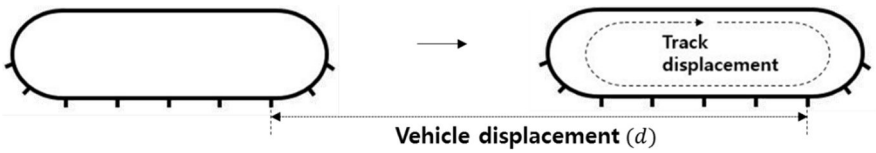


**Figure 2.1 Tracked vehicle travel on paved load**

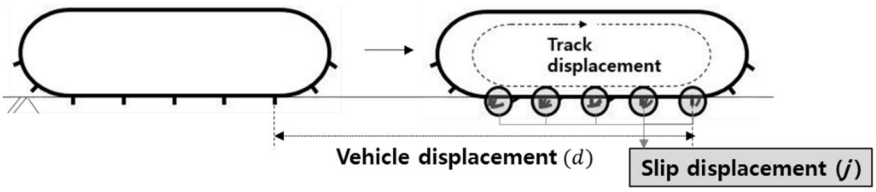


**Figure 2.2 Tracked vehicle travel on off-road**

The shearing behavior of the terrain is therefore one of the major factors determining the tractive performance of an off-road vehicle (Wong and Huang, 2006). A shearing action takes place on the soil-track interaction, which results in the development of slip displacement and soil thrust. And then soil thrust generated by the soil-track interaction acts as a traction.

Soil thrust is traction force induced on the bottom and the side of track. Especially side thrust generated by grouser, which becomes more significant with the increase of grouser height.

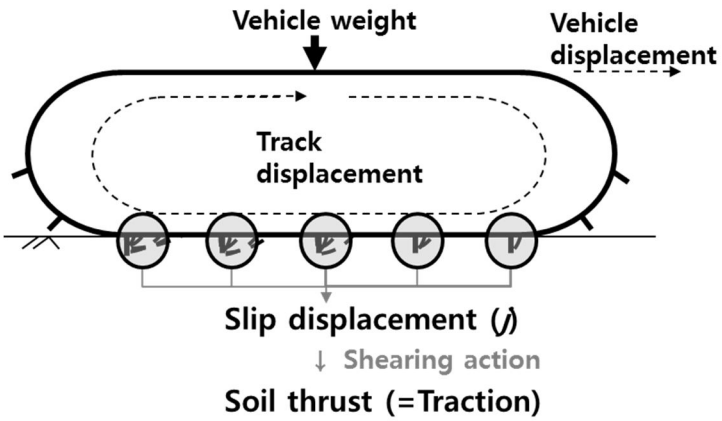


**Figure 2.3 Thrust-slip diagram on the soil-track interface**

Soil thrust increase with slip displacement and approaches a constant value (maximum soil thrust). After reaching at the maximum soil thrust, shear failure occurs within the soil-track interface leading to vehicle idling.

Evaluation of soil thrust-slip displacement relationship is a key factor to assess the off-road vehicle performance. Major factors affecting off-road

vehicle performance are shear strength parameters of soil, vehicle parameters and track system configuration etc. So, theoretical model for evaluating soil thrust-slip displacement relationship needs to be established.

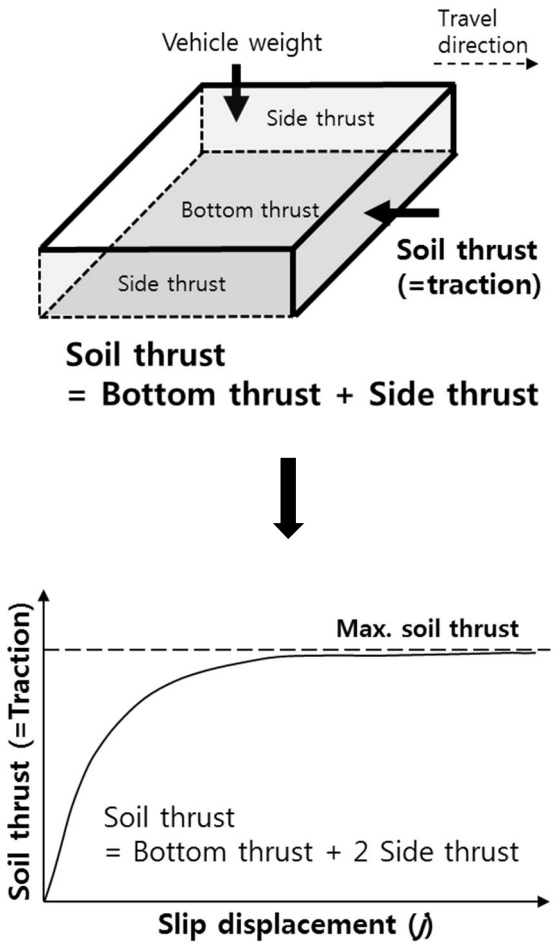


**Figure 2.4 Traction(Thrust)-slip curve of single track system**

## 2.3 Existing Theoretical Model

### 2.3.1 Shear Plane Theory

In shear plane theory, soil thrust–slip displacement described as generation in two different ways: (a) through the horizontal soil compression and distortion and (b) through the soil shear stress–shear deformation in the failure plane (Bekker, 1956). And soil thrust-slip displacement relationship based on the shear stress-shear displacement relationship in a continuous shear failure plane. So, shear stress was defined as a function of slip displacement, obeyed the Mohr-Coulomb criterion. It can be described that soil trust depends on the integral of shear stress ($\tau_s$) times elementary sheared area.

$$\text{Soil thrust} = \int (shear\ stess)$$
$$= \int \tau_b dA_b + 2 \int \tau_s dA_s \tag{2.1}$$

where, $\tau_b$, $\tau_s$ : shear stress on the bottom and on the side

$A_b$, $A_s$ : contact area on the bottom and on the side

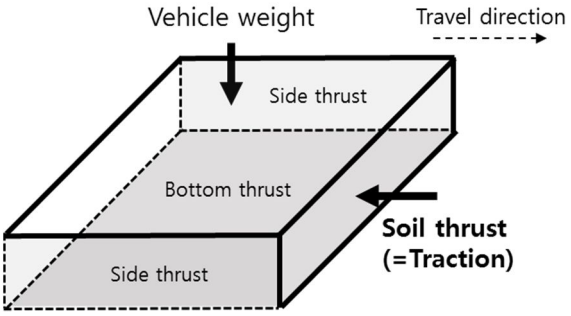


**Figure 2.5 The component of soil thrust for single grouser (Shear plane theory)**

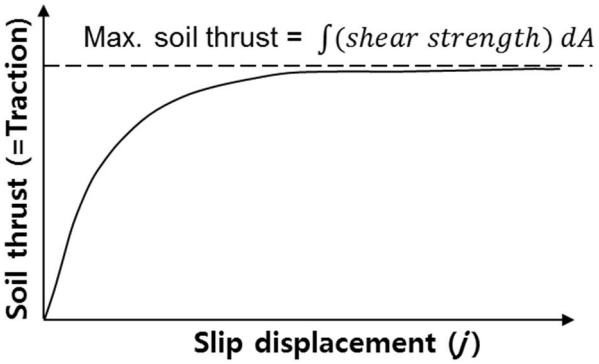


**Figure 2.6 Soil thrust-slip displacement curve (Shear plane theory)**

In shear plane theory, bottom thrust was definitely as;

$$\text{Bottom thrust} = \int (c + \sigma tan\phi)(1 - \exp\left(1 - \frac{j}{K}\right) dA_b \tag{2.2}$$

### 2.3.2 Compression-Sliding Approach

Soil thrust that exerted by soil block compression accompanied by frictional force (compression stage) in Compression-Sliding (CS) approach. Then, soil block is sheared off and slides along the soil-track interface after the transition point (sliding stage). According to Grečenko (2007) in compression stage, the horizontal compression divides the soil into separate soil blocks between any two neighboring grousers and these blocks resist individually the partial horizontal driving forces until their shear strength is reached. In sliding stage, after then, being sheared off start sliding along the soil channel formed by the preceding track sections. The benefit of CS approach is that enables to analyze the effect of track design and loading on the soil thrust-slip displacement characteristics. However how to define maximum soil thrust $(\int(shear\ strength)dA)$ just the same as shear plane theory.

$$\begin{aligned}\text{Soil thrust} &= \text{Soil block compression} + \text{Frictional force} \\ &= F_g/A_g + Wf_t\end{aligned} \tag{2.3}$$

where, $F_g$: compressive force of soil block

$A_g$: contact area on the bottom and on the side

$W$: load of vehicle

$f_t$ : coefficient of friction of soil-track

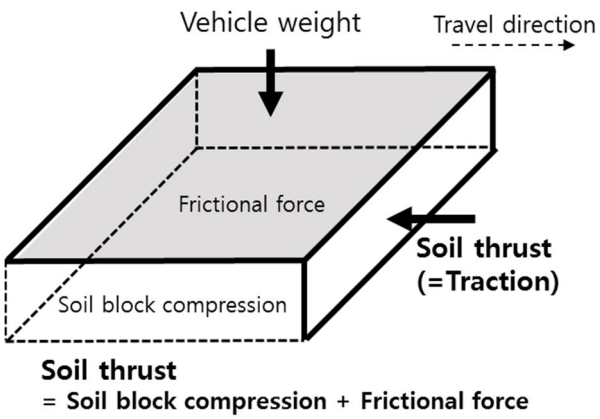


**Figure 2.7 The component of soil thrust for single grouser (CS approach)**

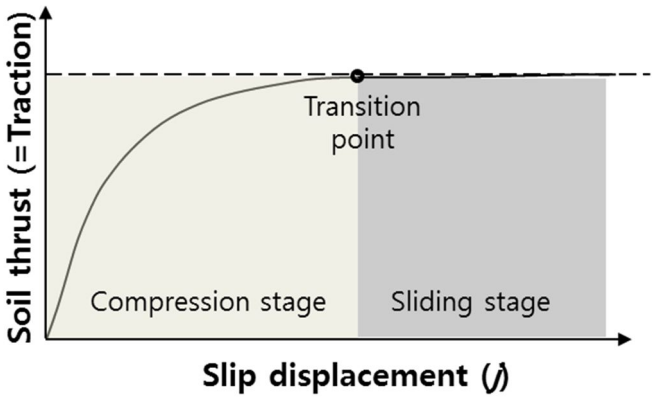


**Figure 2.8 Soil thrust-slip displacement curve (CS approach)**

## 2.4 Conclusions

The method for parametric analysis is useful to consider each force which effect the tracked vehicle. It is essential to assess the relationship between soil thrust and slip displacement based on the soil-track interaction and develop the theoretical model in order to evaluate off-road tracked vehicle performance. Since soil thrust is traction force induced on the bottom and the side of track, both thrust need to be investigated for the prediction of tractive performance. Nevertheless side thrust generated by grouser, which becomes more significant with the increase of grouser height was not fully understood and theoretically defined in previous theoretical models for soil thrust and slip displacement relationship.

**Table 2.1 Existing theoretical model for side thrust**

| Researcher | Shear strength parameters | Shearing surface | Side thrust |
|---|---|---|---|
| Bekker (1956) Wong (1984, 1989) | - | - | - |
| Park et al. (2000) | $c + \sigma_v K_a tan\emptyset$ | Side area $(= hl)$ | $\int (\mathrm{c} + \sigma_v K_a \tan\emptyset)(1 - \exp\left(1 - \frac{j}{K}\right))dA_s$ |
| Grečenko (2007, 2010, 2011) | $c$ | Side area $(= hl)$ | $\int \mathrm{c}(1 - \exp\left(1 - \frac{j}{K}\right))dA_s)$ |

See Table 2.1, Bekker (1956) and Wong (1984, 1989) did not considered side thrust to evaluate the total thrust. Park et al. (2000) assumed that the failure occurred at the side of grouser induced the active earth pressure ($\sigma_v K_a tan\phi$). Actually, failure caused by active earth pressure did not happen when tracked vehicle move towards. And Grečenko (2007) used vertical loads which were too small to generate the friction component of side thrust ($\sigma_h tan\phi$).

The actual process of side thrust generation is shown in Figure 2.9. Failure process like as shallow foundation, did not happen active earth failure with vehicle's vertical load. Actually when vertical load is applied the tracked vehicle, earth pressure that affects inside of the track equals to earth pressure that affects outside of the track. Then, side thrust generate by grouser when the failure occurred and vehicle move forward. The side thrust is expressed by:

$$Side\ thrust = \int Shear\ stress\ dA$$
$$= \int c + (\sigma_h \cdot tan\phi) dA \tag{2.4}$$

$$where,\ \sigma_h = \sigma_v \cdot K_s$$
$$\sigma_v = (F_{axial}\ /A) + \sigma_{mid.soil}$$

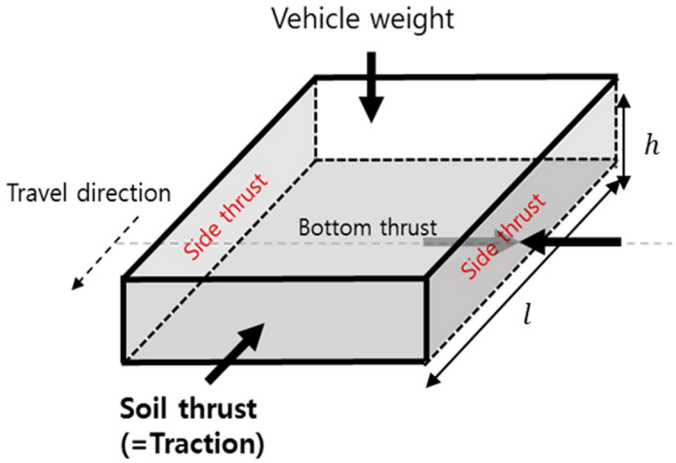


**Figure 2.9 Process of side thrust generation**

# Chapter 3 Experimental Program

## 3.1 Introduction

A series of model track tests were performed on a model track made of stainless steel to examine its side thrust under relative densities 40%. Test procedure can be summarized as:

(1) Prepare model ground with predetermined relative densities (measuring cone index)
(2) Trim the ground to the required shape of soil channel & place a model track system
(3) Apply surcharge mass and lateral load to the model track system with load & displacement measurements

Summarized the process is shown in Figure3.1. Gwan-ak weathered residual soil with relative densities of 40% was trimmed as both soil channel and soil block so as to separate side thrust from total soil thrust. A model track was placed on soil channel or soil block and subjected to surcharge mass and lateral load corresponding to vehicle weight and soil thrust respectively.

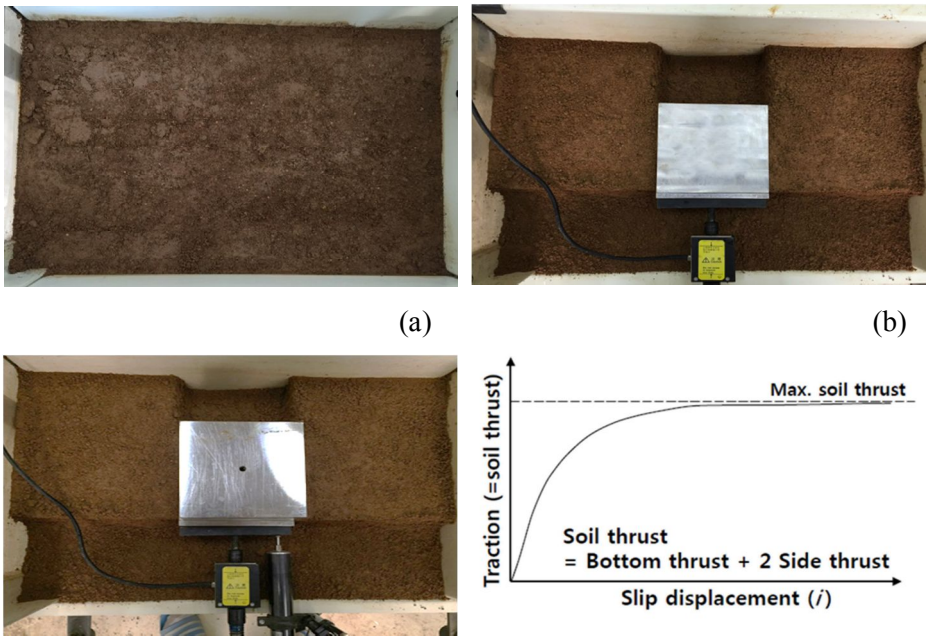


**Figure 3.1 Model track test procedure; (a) model ground, (b) trim the ground and place a model track system (c), apply surcharge mass and track system with load and displacement measurements (d) soil thrust-slip displacement curve from experimental data**

Model ground was trimmed when measuring the total thrust which can be generate thrust both bottom and side of track system. And model ground was trimmed when measuring the bottom thrust which can be generate thrust only bottom of track system.

(a) (b)

**Figure 3.2 Trimmed shape of soil block;**
**(a) Total thrust, (b) Bottom thrust**

## 3.2 Testing Device and Materials

Figure 3.3 illustrates the schematic diagram of the testing device that consists with test chamber, lateral loading device and cross wall. To measure the thrust and slip displacement in the lateral direction. Soil thrust in lateral direction were measured via load cell and slip displacement and sinkage were measured via LVDT.

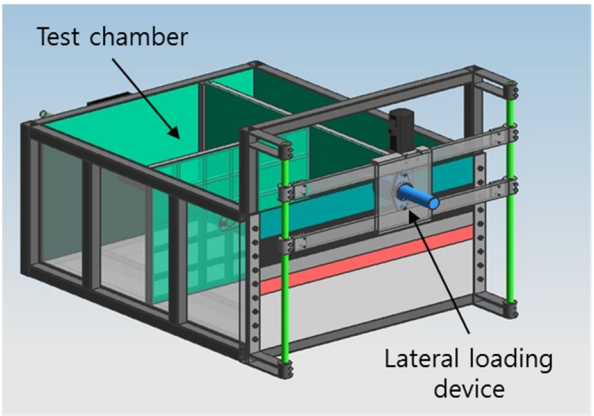


**Figure 3.3 Test chamber and lateral loading device (1000(L) x 800(W) x 500(H) mm)**

**Table 3.1 Lateral loading device**

| | |
|---|---|
| **Max. capacity** | 5kN |
| **Stroke** | 300mm |
| **Loading rate** | 0.1~1 mm/sec |
| **Load cell** | Tokyo sokki (5kN) |

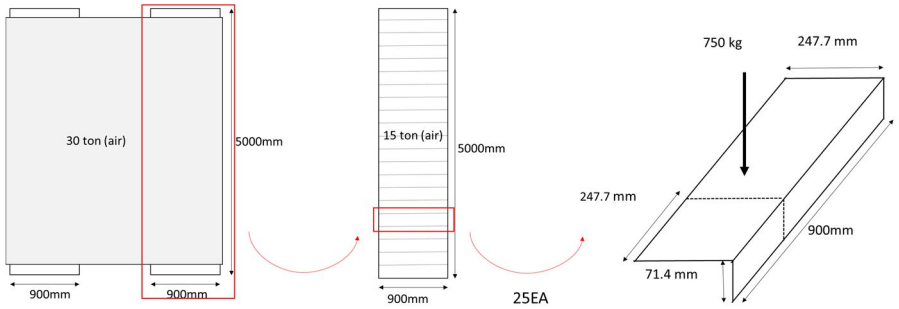


**Figure 3.4 Specification of real track → single grouser**

Common heavy construction vehicle (Volvo 08) (w=30$tonf$, $l$×$d$=5000×900) was selected and scaled down to model track by adopting the Buckingham PI theorem (Figure 3.4). Reducing the length of the track and made a prototype of a square shape due to focus on side thrust generate by grouser and evaluate its effects. Prototype of single track system (Hyundai steel) scale down applied Iai's similitude law (Iai, 1989) with each scaling factors. (Figure 3.6)

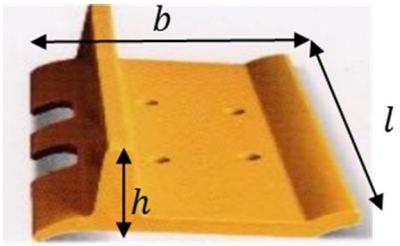


**Figure 3.5 Proto type of single track system (Hyundai steel)**

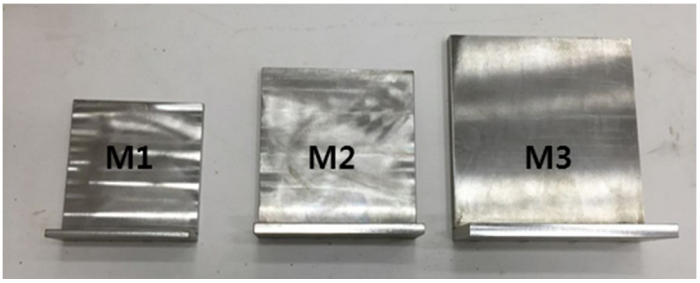


**Figure 3.6 Model track system**

**Table 3.2 Specification of model track**

| | Prototype | M1 | M2 | M3 |
|---|---|---|---|---|
| | | λ =1.3 | λ =1.6 | λ =2 |
| **Geometry ratio, l/h** | 3.47 | 3.47 | 3.47 | 3.47 |
| **Length, l (mm)** | 247.7 | 190.5 | 154.8 | 123.9 |
| **Width, b (mm)** | 247.7 | 190.5 | 154.8 | 123.9 |
| **Height, h (mm)** | 71.4 | 54.9 | 44.6 | 35.7 |
| **Surcharge mass, $F_z$ (kg)** | 137.6 | 62.6 | 33.6 | 17.2 |

Gwan-ak weathered residual soil was manually sampled the Mt. Gwan-ak, Seoul, Korea. Weathered residual soil is classified as well-graded silty sand(SM). Shear strength parameter using in experiment was determined by direct shear tests.

**Table 3.3 Soil properties**

| USCS | $G_s$ | $W_{opt}$ (%) | $D_r$ (%) | $\gamma_d(g/cm^3)$ | c (kPa) | $\phi$ (°) |
|---|---|---|---|---|---|---|
| SM | 2.6 | 12.7 | 40 | 1.4 | 6.1 | 30.7 |

## 3.3 Testing Program

**Table 3.4 Phase of test program**

| Group | Test no. | Grouser | $D_r$ (%) | Ground condition | Vertical load (kg) | v (mm/s) |
|---|---|---|---|---|---|---|
| **G1** | T1 | M1 | 40 | Bottom + Side | 31.3 | 0.07 |
| | T2 | M2 | | | 16.8 | |
| | T3 | M3 | | | 8.6 | |
| **G2** | T4 | M2 | | Bottom + Side | 25.4 | |
| | T5 | | | | 33.6 | |
| | T6 | | | | 16.8 | |
| **G3** | T7 | M2 | | Bottom | 25.4 | |
| | T8 | | | | 33.6 | |

- G1: Verifying the Similitude law to change the model track to real track.
- G2,G3: Evaluating the total thrust and bottom thrust respectively, so from the result to get the side trust under each vertical load.

Soil thrust-slip displacement relationship is function of slip, soil shear parameters, grouser shape, spacing, axial load etc. With the developed test device, track model tests is performed to evaluate the side thrust and tractive performance of tracked vehicle.

# Chapter 4. Experimental Results and Analysis

## 4.1 Verification of Similitude Law

In order to verify the validity of a series of test, conducted a similitude test. Figure 4.2 shows the detailed test conditions.

**Table 4.1 Phase of test program of similitude law**

| Test No. | Grouser | $D_r$ (%) | Ground Condition | Vertical Load (kg) | v (mm /s) |
|---|---|---|---|---|---|
| **T1** | M1 | 40 | Bottom + Side | 31.3 | 0.07 |
| **T2** | M2 | | | 16.8 | |
| **T3** | M3 | | | 8.6 | |

Soil was trimmed as both soil channel and soil block. And using M1, M2, M3 grouser applied the similitude law of $\lambda = 1.3$, $\lambda = 1.6$, $\lambda = 2.0$ respectively. Test results indicated that soil thrust-slip displacement relationship tendency and failure surface on the bottom and side after test.

**(1) T1(M1)**

**(2) T2(M2)**

**(3) T3(M3)**

**Figure 4.1 Failure surface of similitude law test ($D_{r=}40\%$, $\gamma_d = 1.43 g/cm^3$)**

Fig. 4.1 shows the picture of failure surface of similitude law tests result. The failure surfaces of bottom and side thrust were consistent with the grouser shape. And it retains a great similarity regardless of similitude law.

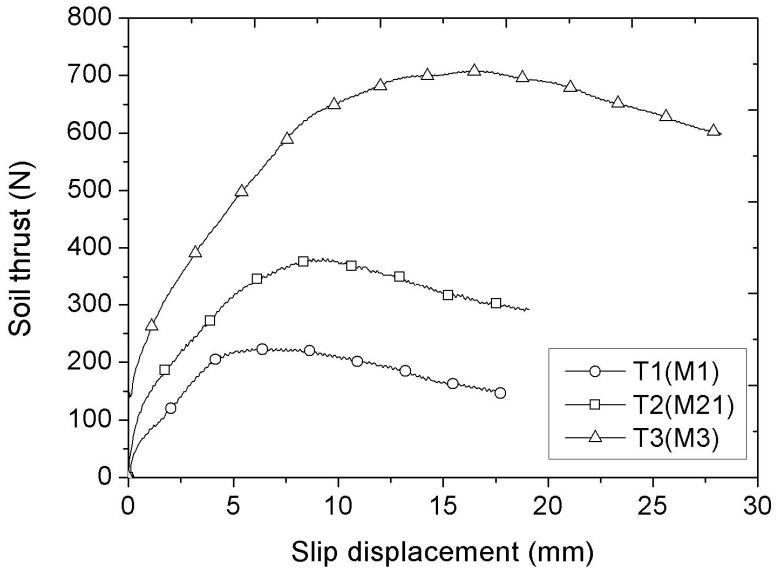


**Figure 4.2 Soil thrust-slip displacement curve of similitude law test**

As shown in Figure 4.2, the soil thrust increase as slip displacement increasing each track model systems. And all of soil thrust-slip displacement relationship showed softening behavior. Figure 4.3 shows the soil thrust-slip displacement curve applied modeling of model method suggested by Kim et al., (2005).

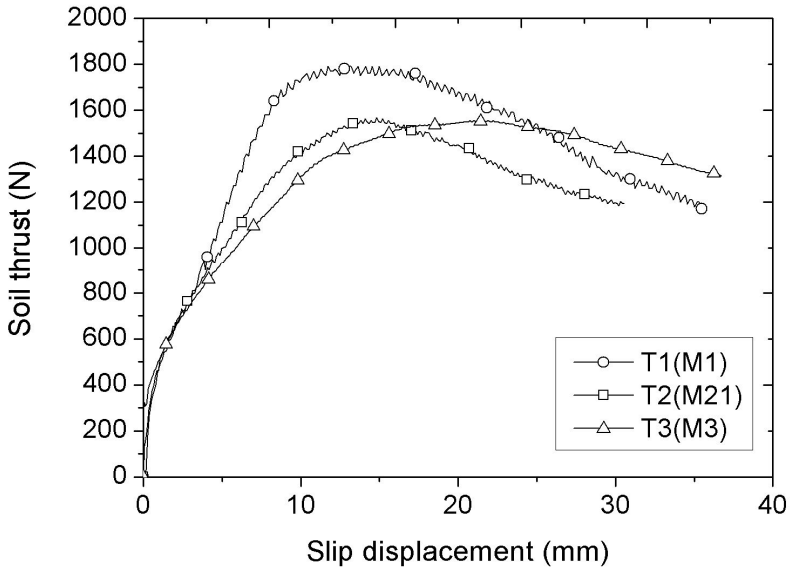


**Figure 4.3 Applied (reverse) similitude law**

To investigate the Fig 4.2, 4.3 experimental results have similar tendencies with prototype results applied reverse similitude law. Particularly, focused on maximum soil thrust, M1=1554.38N, M2=1566.72N, M3=1790.4N in test. M1 and M2 have approximately the same values and M3 is a 10% difference between M1 and M2 but valid values. So, verifying the similitude law is valid.

## 4.2 Assessment of Total Thrust

In order to estimate the total thrust, detailed test conditions are as follows Table 4.2.

**Table 4.2 Phase of test program of total thrust**

| Test No. | Grouser | $D_r$ (%) | Ground Condition | Vertical Load (kg) | v (mm /s) |
|---|---|---|---|---|---|
| **T2** | M2 | 40 | Bottom + Side | 16.8 | 0.07 |
| **T4** | | | | 25.4 | |
| **T5** | | | | 33.6 | |

T2, T4, T5 simulate the vertical load of 10tonf, 15.1tonf, 20tonf respectively. Each vertical load generate on $\sigma \tan\phi$ of shear stress differently. Soil was trimmed as both bottom and side.

Test results indicated that soil thrust-slip displacement relationship tendency and failure surface on the bottom and side after test.

**(1) T2(M2)**

**(2) T4(M2)**

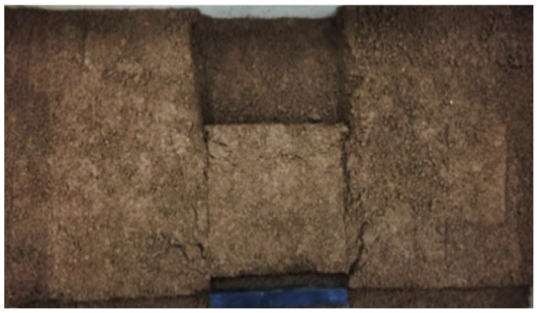

**(3) T5(M2)**

**Figure 4.4 Failure surface of total thrust test ($D_r = 40\%$, $\gamma_d =$**

$1.43g/cm^3$)

Fig. 4.4 shows the picture of failure surface of total thrust test results. The failure surfaces of bottom and side thrust were consistent with the grouser shape. And it retains a great similarity regardless of vertical loads.

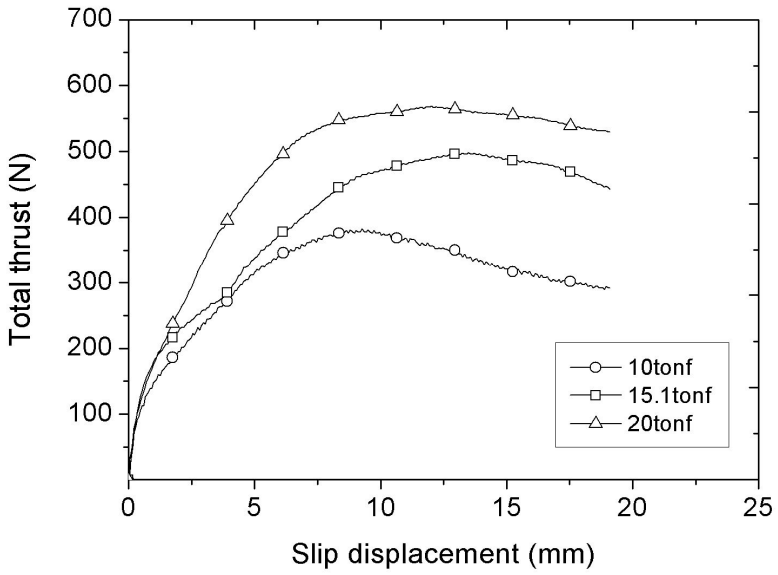


**Figure 4.5 Soil thrust-slip displacement curve of total thrust test**

Figure 4.5 shows the test experimental results of total thrust. An increased of $\sigma\tan\phi$ due to the vertical load leads to increase of the total thrust. In addition, Figure 4.7~9 shows the total thrust which was theoretically evaluated based on the test results and showed good agreement with theoretical predictions each vertical load. And all of soil thrust-slip displacement relationship showed softening behavior.

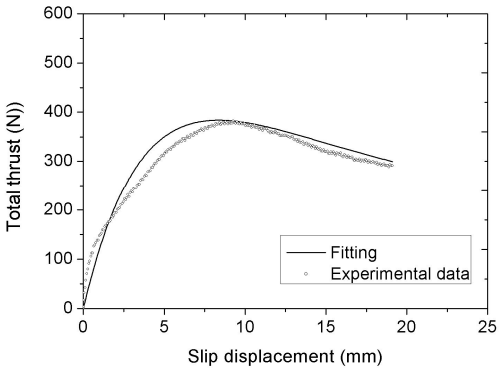


**Figure 4.6 Fitted total thrust-slip displacement (10tonf)**

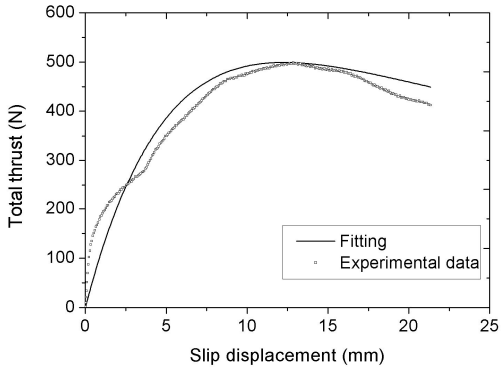


**Figure 4.7 Fitted total thrust-slip displacement (15.1tonf)**

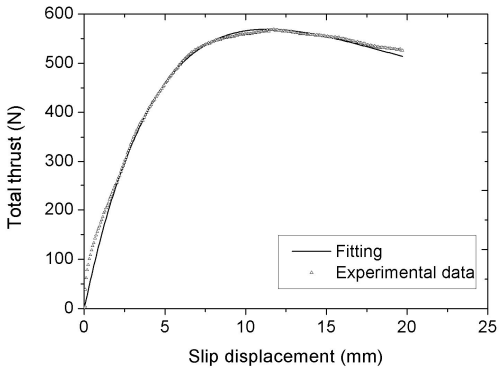


**Figure 4.8 Fitted total thrust-slip displacement (20tonf)**

Total soil thrust-slip displacement relationship were easy and well fitted with softening equation that suggested by Wong (1983) based on experimental data respectively. The strain softening model equation expressed as:

$$\mathrm{F} = F_{max} K_r \left[1 + \left[\frac{1}{K_r\left(1-\frac{1}{e}\right)} - 1\right] \exp\left(1 - \frac{j}{K_w}\right)\right]\left[1 - \exp\left(-\frac{j}{K_w}\right)\right] \tag{4.1}$$

where, $\mathrm{F} = Soil\ thrust$

$\mathrm{j} = \text{slip displacement}$

$F_{max} = max.\ soil\ thrust$

$K_w = 'j'\ where\ F_{max}$ occurs

$K_r = F_{residual}/F_{max}$

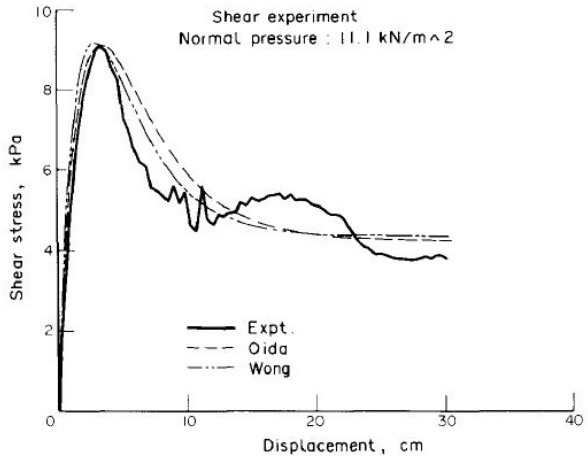


**Figure 4.9 Strain softening model (Wong, 1983)**

Figure 4.10 shows all of experimental data and fitted curve.

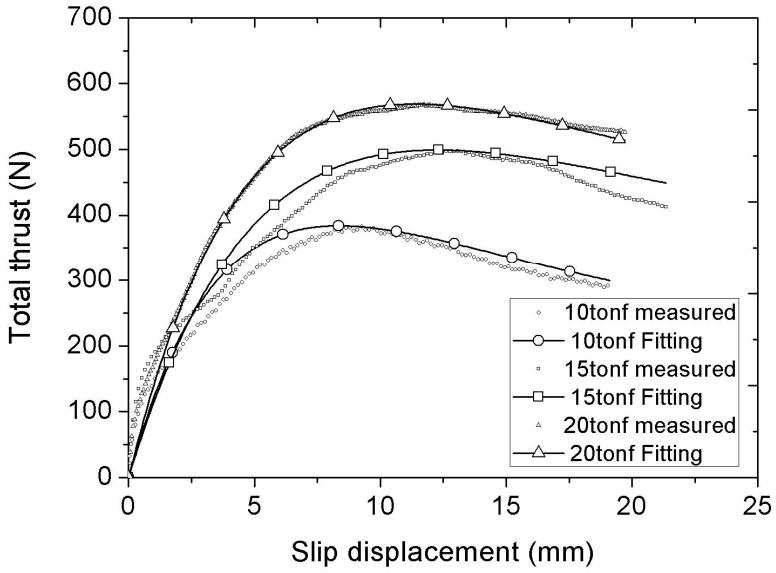


**Figure 4.10 Fitted total thrust-slip displacement**

## 4.3 Assessment of Bottom Thrust

In order to estimate the total thrust, detailed test conditions are as follows Table 4.3.

**Table 4.3 Phase of test program of bottom thrust**

| Test No. | Grouser | $D_r$ (%) | Ground Condition | Vertical Load (kg) | v (mm /s) |
|---|---|---|---|---|---|
| **T6** | M2 | 40 | Bottom | 16.8 | 0.07 |
| **T7** | | | | 25.4 | |
| **T8** | | | | 33.6 | |

T6, T7, T8 simulate the vertical load of 10tonf, 15.1tonf, 20tonf

respectively. Each vertical load generate on $\sigma\tan\phi$ of shear stress differently. In this test condition, only bottom thrust was generated. Test results indicated that soil thrust-slip displacement relationship tendency and failure surface on the bottom of grouser after test.

Fig. 4.4 shows the picture of failure surface of bottom thrust test results. The failure surfaces of bottom thrust were consistent with the grouser shape. And it retains a great similarity regardless of vertical loads.

**(1) T6(M2)**

**(2) T7(M2)**

**(3) T8(M2)**

**Figure 4.11 Failure surface of bottom thrust test ($D_r = 40\%$, $\gamma_d = 1.43 g/cm^3$)**

Fig. 4.11 shows the picture of failure surface of bottom thrust test results. The failure surfaces of bottom thrust were consistent with the grouser shape. And it retains a great similarity regardless of vertical loads.

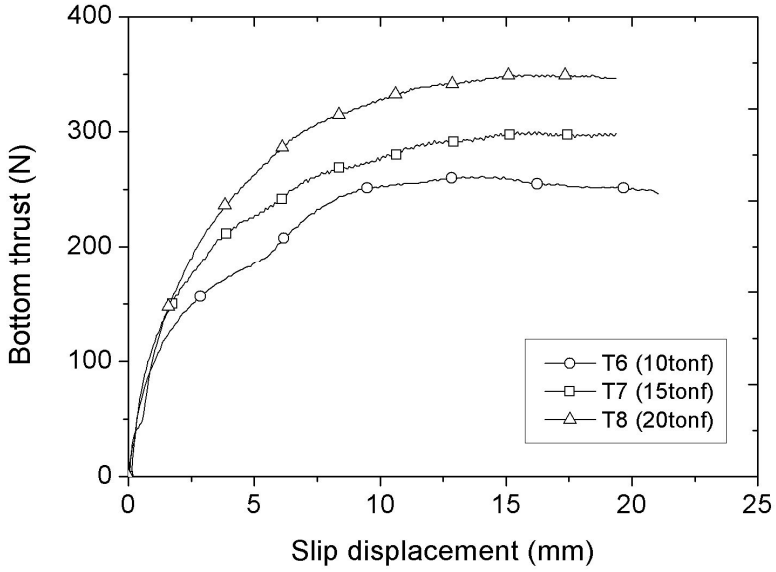


**Figure 4.12 Soil thrust-slip displacement curve of bottom thrust test**

Figure 4.12 shows the test experimental results of bottom thrust. An increased of $\sigma \tan\phi$ due to the vertical load leads to increase of the bottom thrust. In addition, Figure 4.13~15 shows the bottom thrust which was theoretically evaluated based on the test results and showed good agreement with theoretical predictions each vertical load. And all of soil thrust-slip displacement relationship showed hardening behavior.

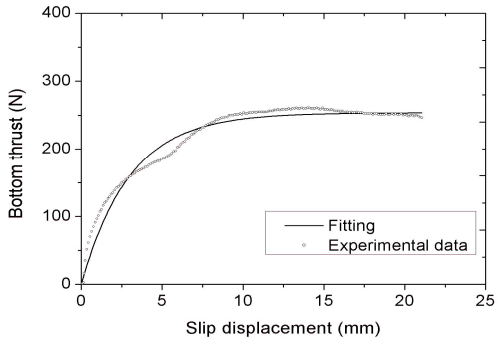


**Figure 4.13 Fitted bottom thrust-slip displacement (10tonf)**

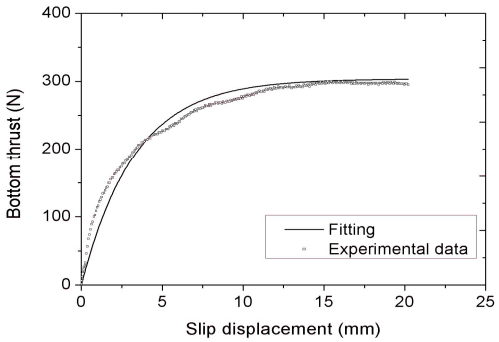


**Figure 4.14 Fitted bottom thrust-slip displacement (15.1tonf)**

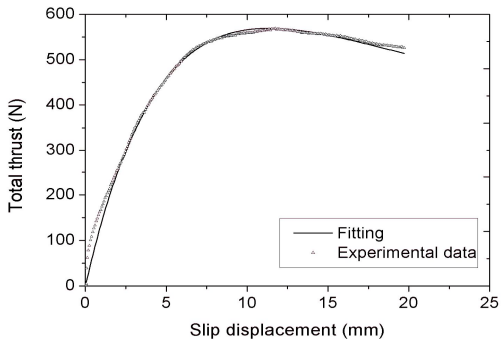


**Figure 4.15 Fitted bottom thrust-slip displacement (20tonf)**

Particularly, focused on maximum bottom soil thrust, the measuring efficiency of the theoretical and experimental data showed that fits within 3%.

**Table 4.4 Comparison of the maximum bottom thrust value**

| Test No. | Theoretical values (N) | Experimental values(N) | Measuring efficiency(%) |
|---|---|---|---|
| **T6** | 253.8 | 261.2 | -2.9 |
| **T7** | 303.7 | 300.0 | +1.2 |
| **T8** | 351.4 | 348.8 | +0.7 |

Theoretical maximum bottom thrust can be represented as:

$$F_{\max(bottom)} = \tau_{\max(bottom)} \times A_{bottom} = (c + (\sigma_v tan\emptyset) \times bh \tag{4.2}$$

Bottom soil thrust-slip displacement relationship were easy and well fitted with softening equation that suggested by Janosi and Hanamoto (1961) based on experimental data respectively.

The strain hardening model equation expressed as:

$$F = F_{max}\left[1 - \exp\left(1 - \frac{j}{K}\right)\right] \quad \text{(cf. Average } K = 3.23\text{)} \tag{4.3}$$

where, $F = Soil\ thrust$

$j =$ slip displacement

$F_{max} = max.\ soil\ thrust$

$K = shear\ deformation\ modulus$

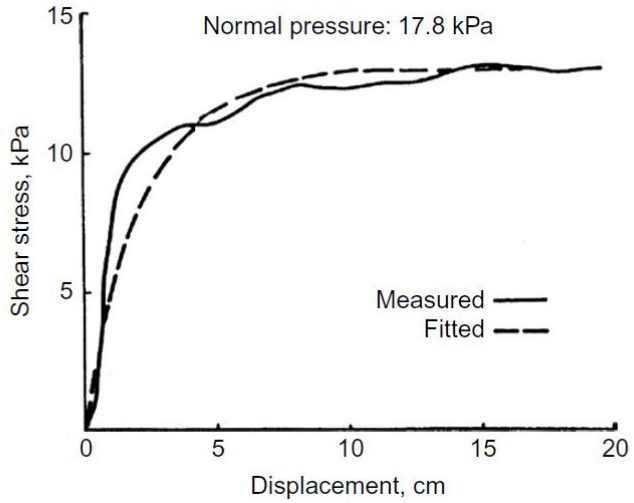


**Figure 4.16 Strain hardening model (Janosi and Hanamoto, 1961)**

To obtain the fitted curve and best value of K for a given set of measured data, the assessed value $F_{max}$ and the procedure based on the weighted least squares method were used.

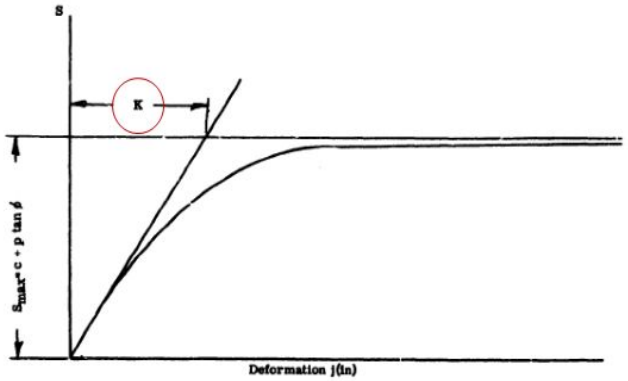


**Figure 4.17 Evaluation of 'K' from a typical soil shear stress-strain curve (Janosi and Hanamoto, 1961)**

## 4.4 Assessment of Side Thrust

In order to estimate the side thrust, detailed test conditions are as follows Table 4.5. Soil thrust was trimmed as both soil channel and soil block so as to separate side thrust from total soil thrust and bottom thrust. So side thrust can be expressed as:

$$\text{Side thrsut} = \text{Total thrust} - \text{bottom thrust} \tag{4.4}$$

**Table 4.5 Phase of test program of side thrust**

| Test No. | Grouser | $D_r$ (%) | Ground Condition | Vertical Load (kg) | v (mm /s) |
|---|---|---|---|---|---|
| **T2** | M2 | 40 | Bottom + Side | 16.8 | 0.07 |
| **T4** | | | | 25.4 | |
| **T5** | | | | 33.6 | |
| **T6** | M2 | 40 | Bottom | 16.8 | 0.07 |
| **T7** | | | | 25.4 | |
| **T8** | | | | 33.6 | |

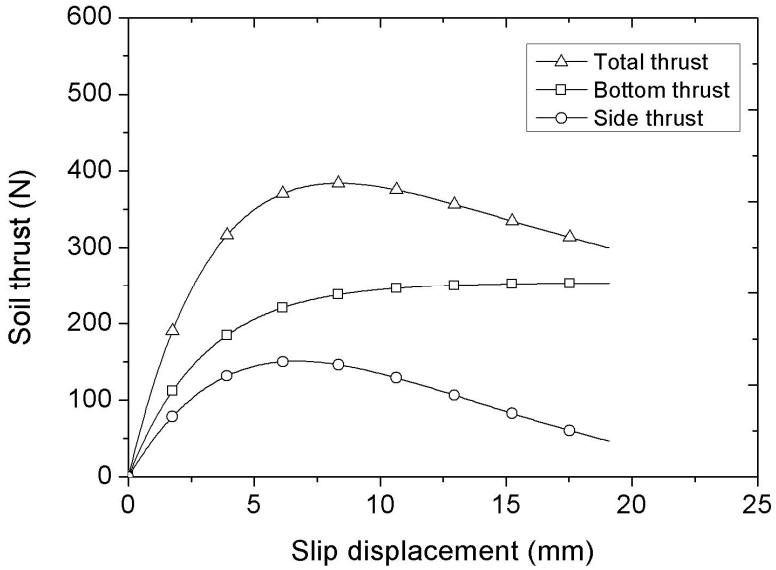


**Figure 4.18 Fitted side thrust-slip displacement (10tonf)**

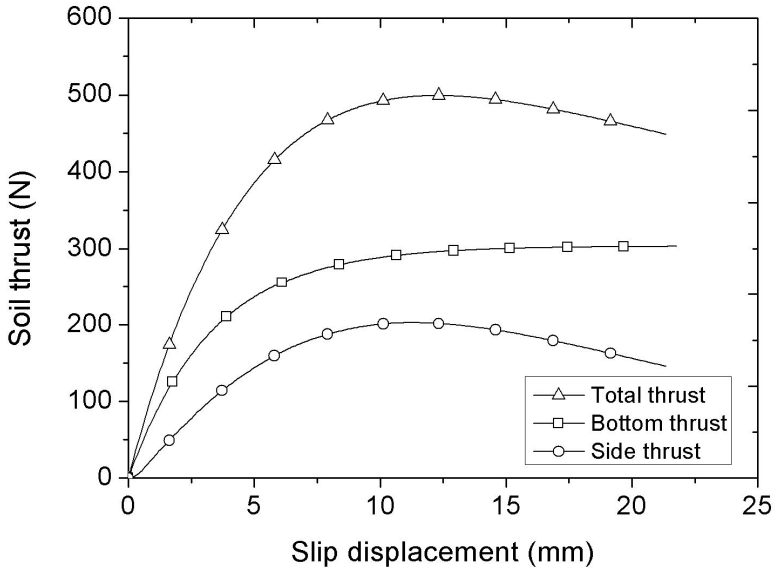


**Figure 4.19 Fitted side thrust-slip displacement (15.1tonf)**

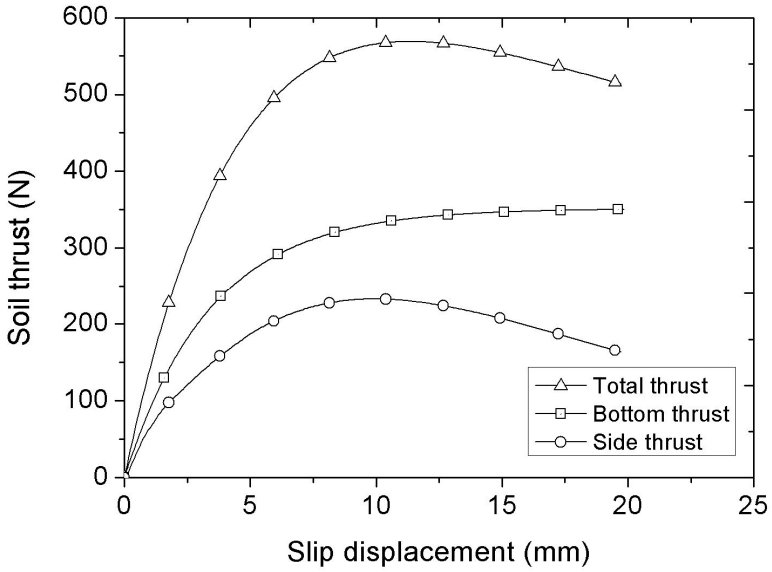


**Figure 4.20 Fitted side thrust-slip displacement (20tonf)**

The failure surface of bottom and side thrust were similar to the direct shear test. So, side thrust depends on the integral of shear stress ($\tau_s$) times elementary sheared side area.

Theoretical maximum thrust can be represented as:

$$F_{\max(side)} = 2 \times \tau_{\max(side)} \times A_{side} = 2 \times (c + \sigma_v K_s tan\emptyset) \times lh \quad (4.5)$$

The coefficient of earth pressure $K_s$ is calculated in case of three different vertical load according to $\sigma_v$.

**Table 4.6 Coefficients of earth pressure $K_s$ according to vertical load**

| Vertical Load | | Mid. Soil stress ($kN/mm^2$) | Total vertical stress $kN/mm^2$) | $K_s$ |
|---|---|---|---|---|
| **Load(kgf)** | **Stress ($kN/mm^2$)** | | | |
| **16.8** | 6.87 | 0.35 | 7.22 | 1.12 |
| **25.4** | 10.39 | | 10.74 | 1.37 |
| **33.6** | 13.74 | | 14.09 | 1.29 |
| **Average $K_s$ values = 1.26** | | | | |

See Table 4.6, there is no difference with the coefficient of earth pressure $K_s$ in terms of each vertical load. So $K_s$ depends on the angle of friction $\phi$ probably. And $K_s$ and coefficients of punching shear resistance in the respect that they are both located between $K_0$ and $K_p$ ($K_0$=0.49, $K_p$=3.08).

Especially, focused on maximum side thrust, the error of the theoretical and experimental data showed that fits within 5%. Additionally compared with previous studies are shown in Figure 4.18 and Table 4.7. See Figure 4.18 and Table 4.7 show the compared with the maximum side thrust value of the previous researcher, the experimental data is most similar to the proposed value. In this regard, it is highly probable that assess the side thrust through the coefficients of earth pressure $K_s$.

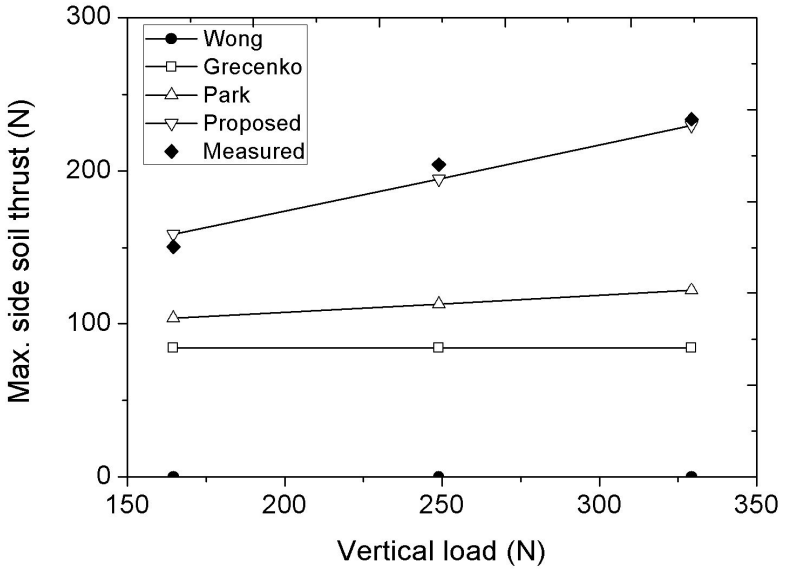


**Figure 4.21 Compared with previous studies and measured data for side thrust**

**Table 4.7 Comparison of the maximum side thrust value**

| Prototype (tonf) | Vertical Load(N) | Theoretical values(N) | Experimental values(N) | Measuring efficiency(%) |
|---|---|---|---|---|
| **10** | 16.8 | 158.7 | 150.8 | +4.9 |
| **15.1** | 25.4 | 195.0 | 204.2 | -4.7 |
| **20** | 33.6 | 229.6 | 233.7 | -1.8 |

Meanwhile, assessed coefficient of earth pressure $K_s$ is similar to $K_s$ (punching shear coefficients) from punching shear theory (Meyerhof, 1974) in shallow foundation. Meyerhof (1974) discussed that, when punching shear

failure occurs, the punching shear coefficient ($K_s$) depends on angle of friction. And the punching shear coefficients $K_s$ is located between $K_0$ and $K_p$.

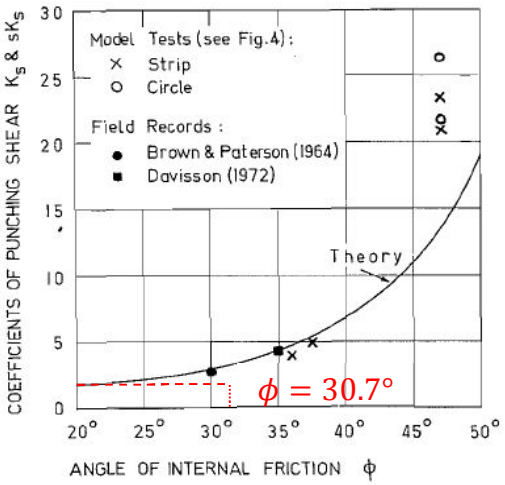


**Figure 4.22 Coefficients of punching shear resistance under vertical load (Meyerhof, 1974)**

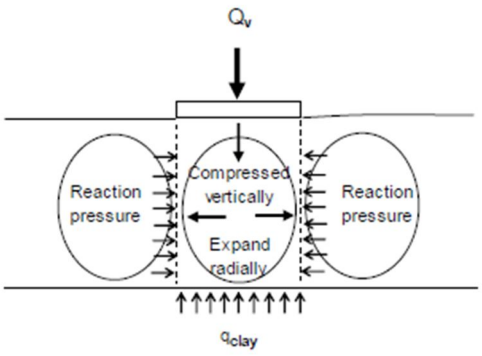


**Figure 4.23 Diagram of reaction forces generated during surface loading (Teh Kar Lu, 2007)**

So, it is necessary to make function in terms of angle of frictions for general application by performing tests under other soil conditions (relative density of 60% and 80%)

# Chapter 5 Conclusions

It is essential to assess the relationship between the soil thrust and the slip displacement based on the soil-track interaction, and to develop a theoretical model for evaluating off-road tracked vehicle performance. As the soil thrust is a traction force induced on the bottom and sides of a track, both thrusts need to be investigated for the prediction of the tractive performance. Nevertheless, the side thrust generated by the grouser, which becomes more significant with the increase of the grouser height, was not fully understood and theoretically defined in the previous theoretical models for the soil thrust-slip displacement relationship. As such, a model track test device was designed and a series of model track tests were performed on a model track made of stainless steel to examine its side thrust, using Gwan-ak residual soil under a 40% relative density. The side thrust was especially focused on.

Through experimental observations, the soil thrust-slip displacement curve was theoretically evaluated, and based on the test results, a theoretical prediction was made. Moreover, the sides were different from those in the previous theoretical model. The side thrust-slip displacement relationship showed a softening behavior. The failure surfaces of the bottom and side thrusts were similar to the punching shear failure and were consistent with the grouser shape.

The coefficient of earth pressure $K_s$ $K_s$ probably depends on the angle of friction co, and $K_s$ is probably located between $K_0$ and $K_p$.

Additional studies are recommended to supplement this research.

*Performing the track model test under an 80% relative density*

(1) A series of model track tests will be carried out under an 80% relative density for weathered residual soil
(2) Suggestion of a function in terms of the angles of friction for general application by combining the results of the test performed under each relative density condition (40, 80%)

# References

Bekker, M.G., (1956). “Theory of land locomotion”, University of Michigan Press.

Bekker, M.G., (1969). “Terramechanics and off-rod vehicles”, Elsevier Publishers.

Choi, J.S., Hong, S. and Kim, H.W., (2003). “An experimental study on tractive performance of tracked vehicle on cohesive soft soil”, Proceeding of the fifth ocean mining symposium, Tsukuba, Japan, pp.139-143.

Grecenko, A., (2007). “Re-examined principles of thrust generation by a track on soft ground”. Journal of Terramechanics, 44(1), pp.123-131.

Grecenko, A., (2007). “Thrust and slip of track determined by the compression-sliding approach”, Journal of Terramechanics, 44(6)., pp.451-459.

Grecenko, A., (2011). “Compression-Sliding approach: Dependence of transitional displacement of a driving element on its size and load”, Journal of Terramechanics, 48(5)., pp.325-332.

Hong, S., Choi, J.S., (2001). “Experimental study on grouser shape effects on trafficability of extremely soft seabed”, Proceeding of the fourth ocean mining symposium, Szczecin, Poland, pp.115-121.

Iai, (1989). “Similitude for shaking table tests on soil-structure-fluid modeling 1g gravitational field”, Soil and Foundation, 29(1), pp.105-

118.

Janosi, Z., Hanamoto, B., (1961). “The analytical determination of drawbar pull as a function of slip for tracked vehicles in deformable soils”, Proceeding of the 1st International Conference on the Mechanics of Soil Vehicle Systems, Edizioni Minerva Tecnica, Torono, Italy.

Karafiath, L.L., Lowatzki, E.A., (1978). “Soil mechanics for off-road vehicle engineering”, Trans Tech Publications.

Liu, J., Gao. H. and Deng, Z., (2008). “Effect of straight grousers parameters on motion performance of small rigid wheel on loose sand”, Information Technology Journal, 7(8), pp.1125-1132.

Meyerhof, G.G., (1974). “Ultimate bearing capacity of footing on sand layer overlying clay”, Canadian Geotechnical Journal, 11(2), pp.223-229.

Moreland, Skonieczny, Inotsume and Wettergreen, (2012). “Soil behavior of wheels with grousers for planetary rovers”, Proceedings of the 2012 IEEE aerospace conference, Boston, MA, USA, pp.1-8.

Teh Kar Lu (2007). “Punching-through of spudcan foundation in sand overlying clay”, National University of Singapore

Wong, J.Y., and Reece, A.R., (1966). “Soil failure beneath rigid wheels”, Proceeding of the 2nd International Conference pf the International Society for Terrain-Vehicle System, 425-445

Wong, J.Y., Preston-Thomas, J. (1983). “On the characterization of the shear stress-displacement relationship of terrain”, Journal of Terramechanics, 19(4)., pp.225-234.

Wong, J.Y., Garber M. and Preston-Thomas J., (1984). “Theoretical prediction and experimental substantiation of the ground pressure distribution and tractive performance of tracked vehicles”, Proceedings of the Institute of Mechanical Engineers, 198D(15):265-285.

Wong, J.Y., (1989). “Introduction to terrain vehicle system”, University of Michigan Press.

Wong, J.Y., Huang, (2006). “Wheels vs. tracks” – A fundamental evaluation from the traction perspective, Journal of Terramechanics, 43(1), pp.27-42.

김성렬, 황재익, 김명모, (2005), “1g 진동대 실험을 위한 상사법칙의 적용성 검증”, 한국지반공학회논문집, 제20권 제9호 (2004. 12) pp.91-103

박원엽, 이규승, 박준걸, (2000). “그라우저에 의해 발생되는 궤도의 측면추진력 예측”, 한국농업기계학회지, 25(1),

# 초 록

궤도차량의 종류로는 군용 탱크, 건설용, 농업용 기계 등이 있으며 최근에는 해양건설시장의 확대로 인해 수중건설시장이 커짐에 따라 수요가 증가한 수중건설로봇 또한 궤도차량이 이용된다. 20tonf 이상의 높은 중량을 가지고 비교적 연약한 지반을 구동하는 궤도차량의 경우 충분한 구동성능을 확보하기 위하여 접지압을 낮추고 일정량 이하로 침하를 제한하는 것이 중요하다.

일반적으로 포장도로 또는 단단한 지반에서 주행하는 궤도차량의 구동력은 궤도와 지면의 마찰에 의해 발생되며, 차량의 엔진성능에 따라 구동성능이 결정된다. 하지만 비교적 연약한 지반에서 운용되는 야지구동 궤도차량의 구동력은 궤도-지반의 interaction에 의해 결정되고, 차량의 엔진성능이 우수하더라도 궤도와 지반의 접지면에서 발생하는 지반의 침하 및 파괴현상에 의해 엔진의 출력을 모두 유용한 구동력으로 전화할 수 없는 경우가 많다. 즉 야지구동 궤도차량의 구동성능은 엔진성능뿐 아니라 차량이 주행하는 지반의 특성과 궤도 및 그라우저의 형상에 따라 결정된다.

하지만 기존의 연구에서는 야지구동 궤도차량의 구동성능을 평가하는데 있어 궤도-지반의 interaction을 적절히 고려하지 못하였으며, 구동성능을 평가하는데 중요한 지반추력-슬립변위 관계에서 필수적인 지반강도정수, 트랙시스템 형상을 적절히 고려하지 못하였다는 한계점이 있다. 특히 지반추력으로 활용되는 구동력은 트랙의 저면과 측면에서 모두 발생되어 두 값이 모두 구동성능평가에 활용되어지기 때문에 명확히 규명하는 것이 중요하다. 그럼에도 불구하고 그라우저에 의해 발생되는

측면지반추력은 그 길이에 길어짐에 따라 그 값이 지배적임에도 불구하고 이론적으로 명확히 규명되어 있지 않다는 한계점이 존재한다.

본 연구에서는 야지구동 궤도차량의 구동성능을 평가하기 위하여 궤도모형시험을 수행할 수 있는 궤도모형시험장치를 설계 및 제작하였으며, 특히 기존에 명확히 규명되지 않은 측면지반추력을 평가하는데 초점을 맞추었다. 측면지반추력은 실험에서 구한 전체지반추력에서 저면 지반추력을 분리함으로써 그 값을 구하였으며, 실험값을 이론적인 값과 비교하였다.

**주요어 : 야지구동 궤도차량, 구동성능평가, 지반-궤도 상호작용, 지반추력, 측면지반추력**

**학 번 : 2014-20550**